Elastic metamaterials with fractional-order resonators

Kaczmarek, Marcin B.; HosseinNia, S. Hassan

DOI
10.1007/s13540-023-00220-w

Publication date
2023

Document Version
Final published version

Published in
Fractional Calculus and Applied Analysis

Citation (APA)
Kaczmarek, M. B., & HosseinNia, S. H. (2023). Elastic metamaterials with fractional-order resonators. *Fractional Calculus and Applied Analysis*, *26*(6), 2522-2539. https://doi.org/10.1007/s13540-023-00220-w

Fractional Calculus and Applied Analysis (2023) 26:2522–2539
https://doi.org/10.1007/s13540-023-00220-w

ORIGINAL PAPER

Elastic metamaterials with fractional-order resonators

Marcin B. Kaczmarek[1] · **S. Hassan HosseinNia**[1]

Received: 15 May 2023 / Revised: 18 October 2023 / Accepted: 18 October 2023 /
Published online: 31 October 2023

Abstract

Elastic metamaterials incorporating locally resonating unit cells can create bandgap regions with lower vibration transmissibility at longer wavelengths than the lattice size and offer a promising solution for vibration isolation and attenuation. However, when resonators are applied to a finite host structure, not only the bandgap but also additional resonance peaks in its close vicinity are created. Increasing the damping of the resonator, which is a conventional approach for removing the undesired resonance peaks, results in shallowing of the bandgap region. To alleviate this problem, we introduce an elastic metamaterial with resonators of fractional order. We study a one-dimensional structure with lumped elements, which allows us to isolate the underlying phenomena from irrelevant system complexities. Through analysis of a single unit cell, we present the working principle of the metamaterial and the benefits it provides. We then derive the dispersion characteristics of an infinite structure. For a finite metastructure, we demonstrate that the use of fractional-order elements reduces undesired resonances accompanying the bandgap, without sacrificing its depth.

Keywords Fractional-order control · Vibration control · Elastic metamaterials · Bandgap · Periodic structures

Mathematics Subject Classification 74H10 · 74H45 · 34A08 · 93B52 · 93B55 · 93C80

1 Introduction

Metamaterials are structures with properties beyond those of their constituents, often composed of repeating patterns called unit cells. The term initially emerged from

✉ Marcin B. Kaczmarek
M.B.Kaczmarek@tudelft.nl

S. Hassan HosseinNia
S.H.HosseinNiaKani@tudelft.nl

[1] Department of Precision and Microsystems Engineering, Delft University of Technology, Mekelweg 2, 2628 CD Delft, The Netherlands

the study of structures capable of manipulating waves, that could be used to create perfect lenses, cloaking devices or superabsorbers. In this paper, we focus on mechanical metamaterials for the manipulation of elastic waves. An overview of historical developments as well as methods and trends in the field can be found in [19, 27]. A feature of metamaterials that offers a promising solution for vibration attenuation and isolation is the creation of bandgaps, i.e., ranges of frequencies in which vibrations cannot propagate through a structure. In elastic metamaterials, thanks to the use of locally resonating unit cells in their structure [6], the bandgaps can be created at much longer wavelengths than the lattice size, which is a clear benefit when compared with phononic crystals whose operating principle is described by Bragg scattering [25]. Within the unit cells, not only mechanical resonators but also passive and active electronic elements can be used, which increases the design freedom and scope of possible implementations.

When a finite resonant metastructure is considered, rather than an infinite metamaterial, it is important to examine the modal behavior, especially in the case of low-frequency vibrations [48]. Application of resonators to a finite host structure results not only in the creation of a bandgap but also introduces additional resonance peaks in the response. Dispersion characteristics of a lattice with resonators are related to the modal behaviour of a host structure [45, 46]. The introduction of the resonators leads to the splitting of resonance peaks corresponding to each mode of the host structure, similar to the effect that can be observed in single-mode systems with tuned mass dampers [12]. These additional peaks are located near the bandgap region, thereby compromising the achieved vibration isolation performance. The modes with resonances above the frequency of the bandgap contribute to the additional peaks below the bandgap region and vice versa.

In the majority of elastic metamaterials presented in the literature, second-order resonators are used. This approach simplifies the analysis and design but also results in a tradeoff between the depth of the bandgap region and the creation of unwanted resonance peaks. While pole placement or optimization-based designs have been proposed to address this issue [47, 55], these methods may not provide the necessary insight for the rational design of metamaterials.

In this paper, we investigate the application of fractional-order (FO) resonators in metamaterials and demonstrate that with this approach the tradeoff between the depth of the bandgap and creating unwanted resonance peaks can be relaxed. To facilitate the use of the tools from control theory, unit-cell level dynamics of the metamaterial are presented as feedback interconnection of an element representing the base structure and the resonator. The working principle of the studied metamaterial is demonstrated in an analysis of a single unit cell in isolation. Subsequently, we derive the dispersion characteristics for an infinite metamaterial structure. To confirm the benefits of the use of FO elements, we investigate vibration transmission through a finite metastructure.

The potential of FO calculus has been demonstrated in various engineering fields. In addition to its use in modelling of electrical, thermal, biomimetic systems, chaos and fractals [5, 17, 33, 44, 50], FO calculus has also been employed in the modelling of viscoelastic materials [2, 3]. Moreover, FO calculus has been found to enhance the performance of controllers, such as FO PID [7, 8, 10, 11], and in the field of active vibration control, FO versions of Integral Resonant Controller (IRC) [14, 40], Positive Position Feedback (PPF) [31, 35], Negative Position Feedback (NPF) [22] and difference feedback for active damping [54] have demonstrated better performance than their integer-order counterparts. In the field of metamaterials, FO operators have been used for the modelling of viscoelastic damping phenomena [4, 13, 26, 43]. In this work, FO resonators of commensurate order [20, 29, 38] as well as power-law generalizations of second-order elements [23, 28, 34, 53] are studied in the context of elastic metamaterials. The theoretical framework provided by FO calculus allows for an extension of the design freedom of a system while preserving the advantages of linearity, making it possible to analytically determine the properties of the system.

The paper is structured as follows. In Section 2, we present background information on FO systems and FO resonators specifically. We also discuss the possible physical implementation of the studied elements. The main contribution of this work is presented in Section 3. First, we revisit a feedback model of an integer order metamaterial. Subsequently, we demonstrate the working principle of the metamaterial with an analysis of a single unit cell in isolation, as well as the derivation of the dispersion relationships of an infinite structure. The analysis of the dynamics of a metastructure with a finite number of unit cells is also conducted. In the concluding Section of the paper, we discuss the obtained results and possible directions for further research.

2 Background

2.1 Fractional-order systems

Fractional-order calculus has been developed to generalize conventional differentiation and integration to non-integer orders [34]. While there exists a vast number of definitions of FO operators, we use the Caputo derivative defined as

$$ {}_{C}\mathcal{D}^{\alpha} f(t) \triangleq \frac{1}{\Gamma(m-\alpha)} \int_{0}^{t} \frac{f^{(m)}(\tau)}{(t-\tau)^{\alpha-m+1}} d\tau, \tag{2.1} $$

where $\alpha \in \mathbb{R}^{+}$ is the order of differentiation and m is a positive integer such that $m-1<\alpha<m$.

The Laplace transform of (2.1) is given by

$$ \mathcal{L}\left[{}_{C}\mathcal{D}^{\alpha} f(t)\right] = s^{\alpha} F(s) - \sum_{k=0}^{m-1} s^{\alpha-k-1} f^{(k)}(0). \tag{2.2} $$

Note, that for zero initial condition the Laplace transform of many FO operators is s^{α}, what greatly simplifies the design of FO controllers in the frequency domain.

A continuous-time FO system is given by a transfer function of the form

$$ H(s) = \frac{b_m s^{\beta_m} + b_{m-1} s^{\beta_{m-1}} + \cdots + b_0 s^{\beta_0}}{a_n s^{\alpha_n} + b_{n-1} s^{\alpha_{n-1}} + \cdots + a_0 s^{\alpha_0}}, \tag{2.3} $$

with $a_i, b_i \in \mathbb{R}$. Changing the orders $\alpha_i, \beta_i \in \mathbb{R}^+$ in (2.3) may lead to dramatic changes in the dynamics of a system, for example from low-pass to high-pass filter [35]. For meaningful analysis, the character of an element should be preserved. To assure this, two variants of FO transfer functions presented bellow will be used.

In a commensurate-order system all the orders of derivation are integer multiples of the base order α, i.e. $\beta_k = k\alpha$ with $k \in \mathbb{Z}^+$, so the transfer function (2.3) is given by

$$H(s) = \frac{\sum_{k=0}^{m} b_k (s^\alpha)^k}{\sum_{k=0}^{n} a_k (s^\alpha)^k}, \tag{2.4}$$

and can be presented as a pseudo-rational function $H(\lambda)$ of the variable $\lambda = s^\alpha$

$$H(\lambda) = \frac{\sum_{k=0}^{m} b_k \lambda^k}{\sum_{k=0}^{n} a_k \lambda^k}. \tag{2.5}$$

A power-law [23, 28, 34, 53] fractional-order system is described by a transfer function of the form

$$H(s) = \left(\frac{\sum_{k=0}^{m} b_k s^k}{\sum_{k=0}^{n} a_k s^k} \right)^\alpha. \tag{2.6}$$

The stability of a FO system can be assessed by studying its transfer function [34]. In general, the denominator of (2.3) is not a polynomial and has an infinite number of roots. Among them, a finite number of roots belonging to the principle sheet of Riemann surface will determine the systems stability. The fractional order system is bounded-input bounded-output stable if all of the roots of the denominator that are in the principle Reimann sheet and are not the roots of the numerator have negative real parts [32].

For a commensurate-order system represented by (2.5), the stability condition is

$$|\arg(\lambda_i)| > \alpha \frac{\pi}{2}, \tag{2.7}$$

where λ_i are the roots of the characteristic polynomial in λ [34]. In the case of power-law filters (2.6), the stability is concluded when the poles of the denominator $\sum_{k=0}^{n} a_k s^k$ lie in the left half complex plain [23].

2.2 Fractional-order resonators

In this section, we review the available results relevant to fractional-order generalizations of second-order high-pass filters close to the limits of the stability, which will be used in the remainder of this paper. FO generalization of elementary transfer functions has been a topic of extensive study. Stability conditions, resonance conditions and characteristic frequencies of such filters were analysed in [20, 29, 38]. These results were generalized to systems of non-commensurate order in [21, 56]. The trajectories of marginally stable FO systems were studied in [49]. Closely related results were obtained for mechanical oscillators with components characterized by FO operators [18, 37, 39, 42].

A commensurate order generalization of a second-order high pass filter is given by

$$R_\alpha(s) = \frac{K_R(\frac{s}{\omega_r})^{2\alpha}}{(\frac{s}{\omega_r})^{2\alpha} + 2\zeta_\alpha(\frac{s}{\omega_r})^{\alpha} + 1}, \tag{2.8}$$

where $\alpha \in (0, 1)$ denotes the order of the pseudo-poles of the system. The FO resonator (2.8) can be represented by a pseudo-rational transfer function

$$R_\alpha(\lambda) = \frac{K_R/\omega_r^{2\alpha}\ \lambda^2}{1/\omega_r^{2\alpha}\ \lambda^2 + 2\zeta_\alpha/\omega_r^{\alpha}\ \lambda + 1}, \tag{2.9}$$

with $\lambda = s^\alpha$, which is characterised by conjugate pair of pseudo-poles at

$$p_\alpha = -\zeta_\alpha\omega_r^\alpha \pm \mathrm{j}\omega_r^\alpha\sqrt{1-\zeta_\alpha^2}. \tag{2.10}$$

The stability condition (2.7) states, that the roots of a stable fractional-order transfer function must lie outside of a closed angular sector. For $\alpha = 1$ this condition is equivalent to the roots remaining in the left half complex plain and can only be satisfied with positive damping coefficients. For $\alpha \in (0, 1)$, the stability region is larger and the transfer function (2.8) is stable for $\zeta_\alpha > -\cos(\frac{\pi}{2}\alpha)$ [29]. This leads to greater design freedom and allows for maintaining a high resonance peak for transfer functions with $\alpha < 1$.

Finding the frequency at which the magnitude response of (2.8) has a maximum in general, involves solving a nonlinear equation [29, 38]. However, for a marginally stable (2.8) the resonance frequency always matches ω_n [29]. This allows us to derive simple approximations useful in the "lightly-damped" case. The resonance peak can be measured by a quality factor Q, determined by the maximum value of the peak, relative to the crossing point of the low and high-frequency asymptotes in the frequency response plot [41]. By evaluating the magnitude of (2.8) with the assumption that the fractional-order attenuator has the peak of response at $\omega = \omega_r$ we obtain

$$\begin{aligned} Q_\alpha &= \frac{|R_\alpha(\omega_r)|}{|R_\alpha(\infty)|} \\ * &= \left(\left(2\zeta_\alpha \sin\left(\frac{\pi}{2}\alpha\right) + \sin\left(\pi\alpha\right)\right)^2 + \left(2\zeta_\alpha \cos\left(\frac{\pi}{2}\alpha\right) + \cos\left(\pi\alpha\right) + 1\right)^2\right)^{-\frac{1}{2}}, \end{aligned} \tag{2.11}$$

which reduces to $Q = \frac{1}{2\zeta_\alpha}$ for $\alpha = 1$.

The equivalent damping for an attenuator with fractional order α, that leads to the same Q-factor as for the integer order attenuator with ζ_r is given by

$$\zeta_\alpha = \zeta_r - \cos\left(\frac{\pi}{2}\alpha\right), \tag{2.12}$$

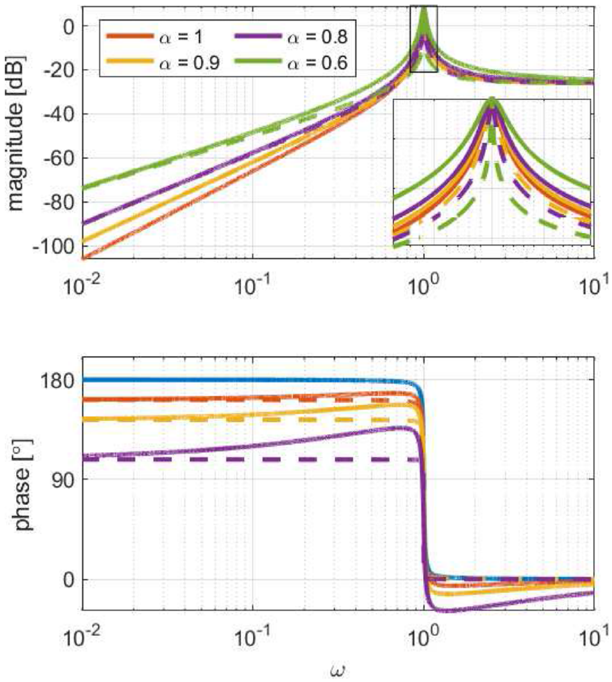

Fig. 1 Frequency responses of commensurate-order (solid lines) and power-law (dashed lines) fractional-order resonators with different values of α. The values of the damping ratio are adjusted to maintain the same quality factor for all compared elements

which is obtained by comparing the quality factor in (2.11) with its integer-order equivalent and finding ζ_α such that both are equal.

The power-law fractional-order generalization of a second-order high-pass filter is

$$\tilde{R}_\alpha(s) = \frac{K_R\left(\frac{s}{\omega_r}\right)^{2\alpha}}{\left(\left(\frac{s}{\omega_r}\right)^2 + 2\tilde{\zeta}_\alpha\left(\frac{s}{\omega_r}\right) + 1\right)^\alpha}, \tag{2.13}$$

which is stable for $\tilde{\zeta}_\alpha > 0$ [23]. Using the same approach as for (2.8), the quality factor and the equivalent damping ratio are defined as

$$\tilde{Q}_\alpha = \frac{1}{(2\tilde{\zeta}_\alpha)^\alpha}, \tag{2.14}$$

$$\tilde{\zeta}_\alpha = \frac{(2\zeta_r)^{1/\alpha}}{2}. \tag{2.15}$$

The frequency responses of integer and fractional-order resonators are compared in Figure 1. The influence of the gain K_R and natural frequency ω_r of the resonator are the same as in the integer-order case. Their change leads to modification of the magnitude and shift of the frequency response along the frequency axis respectively. At low frequencies, the magnitude of the frequency response is proportional to $\omega^{2\alpha}$, which is linked to the phase of $\alpha\pi/2$. This effect, as explained in [22], leads to a lower amplitude of introduced resonance peaks when the element is used for vibration control. In the high-frequency region, all the elements have a constant magnitude of the frequency response and the phase of 0. For the commensurate-order FO element (2.8), decreasing α leads to the widening of the resonance peak. At the same time, the phase close to the resonance frequency exceeds the low and high-frequency asymptotes. The phase of the power-law element (2.13) does not intersect the asymptotes, but the resonance peak narrows down as α is decreased.

2.3 Physical implementation of fractional-order resonators

In active structures with sensors and actuators, the fractional-order resonators can be implemented as controllers with appropriate transfer functions. A common way to implement FO systems is to approximate them in an appropriate range of frequencies using finite-dimensional integer-order transfer functions. An overview of approximation techniques can be found in [52]. In continuous time, expansion-based and frequency-domain identification methods can be used to find the approximation. In the latter category, the approximation can be found analytically, like in the method of Oustaloup [36], or identified directly from the desired frequency response using commercial software. While direct discrete-time approximations of FO systems exist, it is also possible to discretise a continuous-time approximation, which yields satisfactory results if the sampling ratio is sufficiently high.

Alternatively, the fractional-order resonators can be implemented by shunting the transducers present in the structure with electronic components with FO dynamics. In [1, 51] the direct implementation of electronic resonators was studied. To the best of authors' knowledge, passive mechanical resonators with FO dynamics have not been developed yet. Similarly, emulation of an FO resonator dynamics be a higher number of integer-order resonators remains an open question.

3 Fractional-order metamaterials

In this section, we present the main contribution of the paper and study the application of fractional-order resonators in an elastic metamaterial. First, the dynamics of the system in the integer case are revisited. Second, the working principle is presented in an analysis of the dynamics of a single cell in isolation. Subsequently, we conduct the dispersion analysis for an infinite structure. The section concludes with an investigation of vibration transmission through a finite structure.

3.1 System model

Consider the granular metamaterial [16] presented in Figure 2. This choice of simple lumped parameter models allows us to focus on the underlying phenomena free from the distraction of irrelevant system complexities. Each unit cell of the metamaterial consists of a host-structure element with mass m_p connected to neighbour unit cells

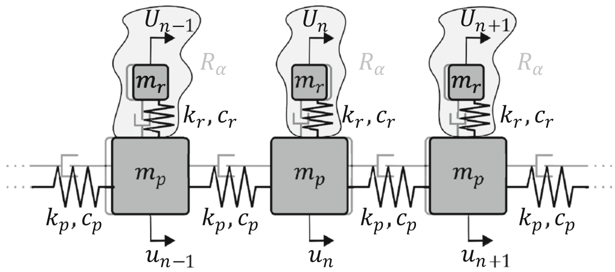

Fig. 2 A chain of masses with resonators. Grey loops indicate the resonators, whose dynamics are extended using fractional-order calculus

by stiffness k_p and viscous damper c_p. To the host element of each unit cell a resonator characterised by mass m_r, stiffness k_r and damping c_r is attached. The dynamics of nth unit cell are described by

$$\begin{aligned} m_p\ddot{u}_n &= k_p(u_{n-1} + u_{n+1} - 2u_n) + k_r(U_n - u_n) \\ &\quad + c_p(\dot{u}_{n-1} + \dot{u}_{n+1} - 2\dot{u}_n) + c_r(\dot{U}_n - \dot{u}_n), \end{aligned} \tag{3.1a}$$

$$m_r\ddot{U}_n = k_r(u_n - U_n) + c_r(\dot{u}_n - \dot{U}_n), \tag{3.1b}$$

where u_n and U_n denote the displacement of the host element and the resonator of nth unit cell. To clearly present the band-gap region, $\omega_r << \omega_p$ is selected. The damping ratio ζ_p is small since it is determined by the host structure and $\zeta_r \approx 0$ is desired to create deep band gaps. By taking the Laplace transform of (3.1) and defining $\omega_p^2 = 2k/m$, $\omega_r^2 = k_r/m_r$, $K_R = k_r/k_p$, $\zeta_p = 2c_p/2\sqrt{2k_p m_p}$, $\zeta_r = c_r/2\sqrt{k_r m_r}$ we obtain

$$\begin{aligned} &\left(\left(\frac{s}{\omega_p}\right)^2 + 2\zeta_p\left(\frac{s}{\omega_p}\right) + 1 + \frac{1}{2}\frac{K_r\left(\frac{s}{\omega_r}\right)^2\left(2\zeta_r\left(\frac{s}{\omega_r}\right)+1\right)}{\left(\frac{s}{\omega_r}\right)^2 + 2\zeta_r\left(\frac{s}{\omega_r}\right)+1}\right)u_n(s) \\ &= \frac{1}{2}\left(u_{n-1}(s) + u_{n-1}(s)\right), \end{aligned} \tag{3.2}$$

with $u_i(s)$ denoting Laplace transform of the signal u_i. The dynamics between neighbour unit cells can be represented as

$$u_n = Tu_{n-1} + Tu_{n+1}, \tag{3.3a}$$

$$T(s) = \frac{u_n(s)}{u_{n-1}(s)} = \frac{u_n(s)}{u_{n+1}(s)} = \frac{P(s)}{1 + P(s)R(s)} = P(s)S(s), \tag{3.3b}$$

$$P(s) = \frac{\frac{1}{2}}{\left(\frac{s}{\omega_p}\right)^2 + 2\zeta_p\left(\frac{s}{\omega_p}\right) + 1}, \tag{3.3c}$$

$$R(s) = \frac{K_R(\frac{s}{\omega_r})^2\left(2\zeta_r\left(\frac{s}{\omega_r}\right)+1\right)}{\left(\frac{s}{\omega_r}\right)^2+2\zeta_r\left(\frac{s}{\omega_r}\right)+1}, \tag{3.3d}$$

which can be related to the "vibration reduction ratio" concept [24].

In the remainder of the paper, we study the effects that replacing the resonator (3.3d) with FO counterparts (2.8) and (2.13). The transfer function (3.3d) describes the relation between the displacement of the main body of the unit cell u_n and the force applied on it due to the presence of the resonator. For lightly damped resonators, the zero at $s = -\omega_r/(2\zeta_r)$ can be neglected, so the proposed FO generalization is justified.

3.2 Single unit-cell analysis

To demonstrate the root cause of the tradeoff between attenuation of vibrations in the bandgap and amplification at unwanted resonance peaks, as well as the proposed solution, consider the nth unit cell in isolation, driven by displacement n_{n-1} and with $u_{n+1} = 0$. If a fractional-order resonator (2.8) is used, the transmissibility (3.3b) is given by

$$T = \frac{\frac{1}{2}\left(\left(\frac{s}{\omega_r}\right)^{2\alpha}+2\zeta_\alpha\left(\frac{s}{\omega_r}\right)^{\alpha}+1\right)}{\left(\left(\frac{s}{\omega_r}\right)^{2\alpha}+2\zeta_\alpha\left(\frac{s}{\omega_r}\right)^{\alpha}+1\right)\left(\left(\frac{s}{\omega_p}\right)^{2}+2\zeta_p\left(\frac{s}{\omega_p}\right)+1\right)+\frac{1}{2}K_R\left(\frac{s}{\omega_r}\right)^{2\alpha}}, \tag{3.4}$$

with $\alpha = 1$ representing the integer-order case. The response of the unit cell is characterized by a pair of pseudo-zeros at the location of the resonator poles p_α (2.10), which are related to the creation of a band gap in the metamaterial. The denominator of (3.4) contains terms with different fractional order, which complicates the analysis. In order to enable pseudo-pole analysis, $P(s)$ and $R(s)$ will be approximated at different frequency ranges.

Recall that $\omega_r < \omega_p$ are selected. At frequencies $\omega >> \omega_r$ the response of the resonator with any value of α can be approximated by the gain K_R. The transmissibility (3.4) is then approximated as

$$T_{\omega>\omega_r} \approx \frac{\frac{1}{2}}{\left(\frac{s}{\omega_p}\right)^2+2\zeta_p\left(\frac{s}{\omega_p}\right)+1+\frac{1}{2}K_R}, \tag{3.5}$$

with poles at $p_{\omega>\omega_r} = -\zeta_p\omega_p \pm j\omega_p\sqrt{1+K_R/2-\zeta_p^2}$. The location of the poles is illustrated in Figure 3a. Since $\zeta_p \approx 0$ we have $\angle p_{\omega>\omega_r} \approx \pi/2$ and a resonance peak with high-quality factor is created. To reduce the height of this resonance peak, the value of ζ_p has to be increased.

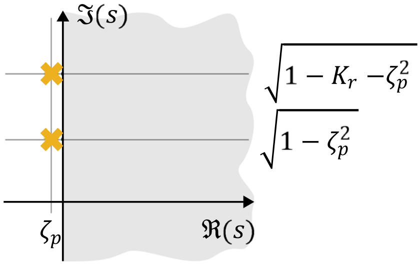

(a) $\alpha=1$, $\zeta_p=0$, $\zeta_r\neq 0$

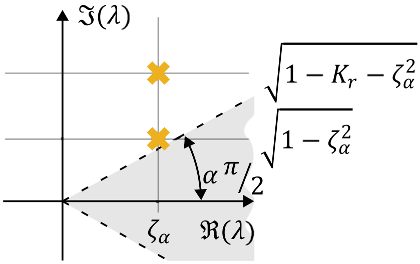

(b) commensurate-order, $\zeta_p = 0$, $\zeta_{r,\alpha=1}=0$

Fig. 3 Locations of approximated (pseudo)poles of a single unit cell for a) $\omega >> \omega_r$ and b) $\omega \approx \omega_r$ or $\omega < \omega_r$. The absolut values of poles are scaled to enable comparison

In the vicinity of ω_r and at lower frequencies, the response of $P(s)$ can be approximated by the gain $\frac{1}{2}$. The transmissibility (3.4) is then approximated as

$$T_{\omega<\approx\omega_r} \approx \frac{\frac{1}{2}\left(\left(\frac{s}{\omega_r}\right)^{2\alpha}+2\zeta_\alpha\left(\frac{s}{\omega_r}\right)^{\alpha}+1\right)}{\left(\left(\frac{s}{\omega_r}\right)^{2\alpha}+2\zeta_\alpha\left(\frac{s}{\omega_r}\right)^{\alpha}+1\right)+\frac{1}{2}K_R\left(\frac{s}{\omega_r}\right)^{2\alpha}}, \tag{3.6}$$

which is characterized by a pair of pseudo-zeros at p_α (2.10) and a pair of poles at $p_{\omega<\approx\omega_r} = \frac{1}{1+K_R/2}\left(-\zeta_\alpha\omega_r^\alpha \pm \mathrm{j}\omega_r^\alpha\sqrt{1+K_R/2-\zeta_\alpha^2}\right)$. From (2.12), for $\alpha = 1$ we have $\zeta_\alpha \approx 0$, so $\angle p_{\alpha|\alpha=1} \approx \angle p_{\omega<\approx\omega_r|\alpha=1} \approx \pi/2$, which means that the low-frequency resonance with high-quality factor is created. The presence of the resonance peak in the response is undesired since the function of a resonant metamaterial is to reduce vibration transmission. The height of the resonance peak can be reduced by increasing ζ_r, by the cost of also reducing the depth of the zero, since the damping of both poles and zeros of the structure increases simultaneously. This illustrates a fundamental tradeoff in elastic metamaterials.

With a fractional-order resonator with $\alpha < 1$, a damped low-frequency resonance peak can be created without affecting the damping ratio of the zero pair, therefore relaxing the aforementioned tradeoff. The pole locations, in this case, are presented in Figure 3b. For $\alpha < 1$, the high-quality factor of the resonator is obtained with $|\zeta_\alpha| > 0$ and the pair of the pseudo-zeros is placed close to the stability margins $\angle p_\alpha \approx \alpha\pi/2$. Simultaneously, $\angle p_{\omega<\approx\omega_r|\alpha<1} > \angle p_\alpha$ as the poles of the transmissibility are moved deeper into the stable region. A similar effect is expected for power-law resonators (2.13), however, the pseudo pole analysis in not possible due to the definition of resonator's dynamics.

The influence of commensurate-order and power-law FO resonators with different orders α on the transmissibility of a single unit cell is presented in Figure 4. For all the elements, a zero in transmissibility is created at ω_r and the same attenuation of vibration transmission at this frequency is obtained, as it is related to the location of (pseudo)zeros in the complex plain. The bandwidth at which the influence of the zeros

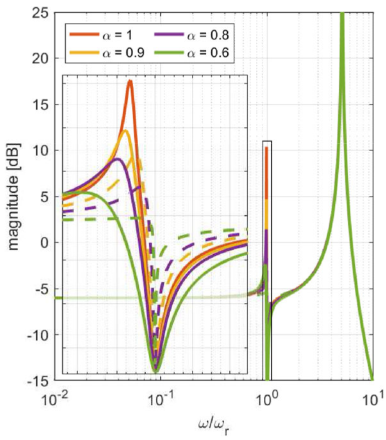

Fig. 4 Infuence of α on the transmissibility of a single unit cell for resonators with commensurate-order (solid lines) and power-law (dashed lines) definitions. The damping of all the resonators is adjusted to maintain the same quality factor

is visible increases with decreasing α for commensurate-order resonators. For the power-law FO resonators decreasing α has the opposite effect, which can be related to the width of resonance peaks of (2.8) and (2.13). The benefit of the use of FO resonators is visible in the height of the resonance peak below ω_r. As α is decreased, the height of the resonance peak is decreased for both types of FO resonators, but the attenuation is significantly stronger in the power-law case. In the high-frequency region, if ω_r is sufficiently smaller than ω_p the second resonance peak remains unaffected with all the resonators.

3.3 Dispersion analysis of a fractional-order resonant metamaterial

In this subsection, we analyse the vibration transmission in an infinite elastic metamaterial with fractional order resonators using the dispersion method. Following the Bloch-Floquet theory, the spatial component of the harmonic wave solution for the nth unit cell can be expressed as $u_n(\omega) = \tilde{u}\,(\mu(\omega))\, e^{j\mu n}$, where $\tilde{u}$ defines the amplitude of the wave motion and the exponential term describes the magnitude and phase changes as the wave propagates thru the unit cells [19], with μ denoting the propagation constant. Wave propagation without magnitude change corresponds to real μ, while the imaginary part of μ indicates attenuation of the wave as it progresses thru the lattice. By implementing this in (3.3), considering nontrivial solutions ($\tilde{u} \neq 0$) and taking $s = \mathrm{j}\omega$ we obtain

$$\cos(\mu) = \frac{1}{2T(\omega)}. \tag{3.7}$$

The attenuation factors can be found by solving (3.7) in terms of the propagation constant at given frequencies. The band gaps can be identified as ranges of frequencies in which the propagation constant takes pure imaginary values. A physical interpretation of this problem is related to wave propagation in a medium due to sustained sinusoidal excitation with dissipation limited to spatial attenuation [15].

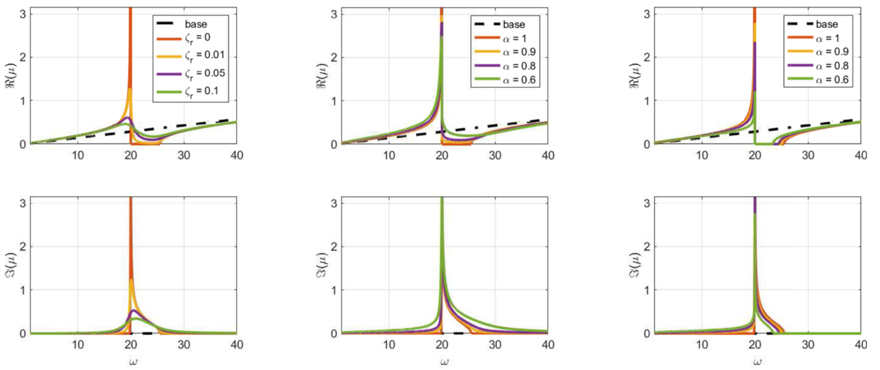

(a) $\alpha = 1$, $\zeta_p = 0$, $\zeta_r \neq 0$ (b) commensurate-order, $\zeta_p = 0$, $\zeta_{r,\alpha=1} = 0$ (c) power-law, $\zeta_p = 0$, $\zeta_{r,\alpha=1} = 0$

Fig. 5 Dispersion diagrams for metamaterials with (a) integer-order and (b) commensurate-order or (c) power-law fractional-order resonators

To create the baseline for the analysis, Figure 5a presents the dispersion diagram of an integer-order metamaterial (i.e. with (2.8), $\alpha = 1$) with $\zeta_p = 0$ and different values of ζ_r. As the value of ζ_r increases, the maximal value of achieved attenuation factor $\Im(\mu)$ decreases, due to the lowering of the quality factor of the resonator. Simultaneously, the range of frequencies with non-zero attenuation increases, which can be used for widening the band-gap region [9, 30]. Moreover, the range of frequencies in which μ takes pure imaginary values disappears. This is caused by the phase of the frequency response of the resonator diverging significantly from the low and high-frequency asymptotes in the vicinity of the resonance peak.

Figure 5b presents a dispersion diagram for metamaterial with commensurate - order resonators and $\zeta_p = 0$, $\zeta_\alpha = -\cos(\alpha\pi/2)$. Since the quality factor of the resonator does not change with changing α, high values of attenuation ratio $\Im(\mu)$ are preserved. However, values for $\alpha < 1$ are slightly lower than in the integer case due to the phase at the resonance lower than 90° [6]. Simultaneously, the width of the frequency range with $\Im(\mu) \neq 0$ increases. Similar to the integer-order case with $\zeta_r \neq 0$, the region of frequencies with pure imaginary μ disappears.

In Figure 5c a dispersion diagram of metamaterial with power-law fractional-order resonators and $\zeta_p = \tilde{\zeta}_\alpha = 0$ is presented. Similar to the commensurate-order case, the high attenuation ratio $\Im(\mu)$ is preserved, with only a slight decrease in maximal magnitude, when α decreases. The range of frequencies with $\Im(\mu) \neq 0$ extends towards lower values thanks to the lower phase of the frequency response of the resonator for $\alpha < 1$, and shrinks in the high-frequency side due to the narrowing of the resonance peak. The phase of the resonator does not extend beyond the high-frequency asymptote, which prevents the expansion of the band gap towards high frequencies. Simultaneously, the same leads to the reappearance of the range of frequencies with $\Re(\mu) = 0$.

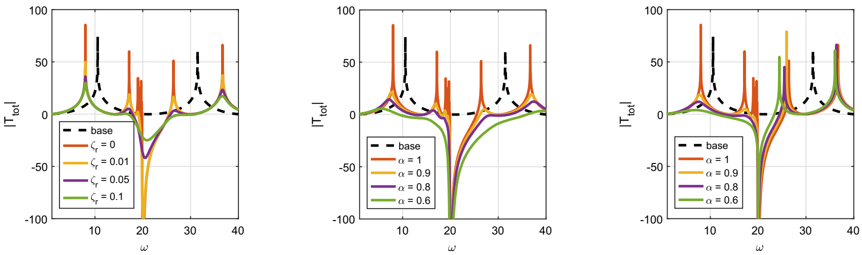

(a) $\alpha = 1$, $\zeta_p = 10^{-6}$, $\zeta_r \neq 0$

(b) commensurate-order, $\zeta_p = 10^{-6}$, $\zeta_{r,\alpha=1} = 10^{-6}$

(c) power-law, $\zeta_p = 10^{-6}$, $\zeta_{r,\alpha=1} = 10^{-6}$

Fig. 6 Transmissablity of a finite metastructure of 10 cells with (a) integer-order and (b) commensurate-order or (c) power-law fractional-order resonators. The base chain of the metastructure is nearly undamped

3.4 Fractional-order resonant metastructure

The effectiveness of the proposed fractional-order resonators for attenuation of undesired resonance peaks in the vicinity of the bandgap region can be fully seen when a finite metastructure is considered. In a finite chain of N cells, the transmission of the vibrations from the base with displacement u_0 to the end of the chain can be calculated using (3.3) and assuming $u_{N+1} = u_N$ to represent the free boundary condition at the end of the chain. The dynamics of the complete resonant metastructure are then represented by

$$\begin{bmatrix} 1 & -T & 0 & \cdots & & \cdots & 0 \\ -T & 1 & -T & 0 & & & \vdots \\ 0 & \ddots & \ddots & \ddots & & & \\ \vdots & & -T & 1 & -T & & \vdots \\ & & & \ddots & \ddots & \ddots & 0 \\ \vdots & & & 0 & -T & 1 & -T \\ 0 & \cdots & & \cdots & 0 & -T & 1-T \end{bmatrix} \begin{bmatrix} u_1 \\ \vdots \\ u_{n-1} \\ u_n \\ u_{n+1} \\ \vdots \\ u_N \end{bmatrix} = \begin{bmatrix} T u_0 \\ \vdots \\ \\ \\ \\ \vdots \\ 0 \end{bmatrix}, \tag{3.8}$$

and transmissability of the complete metastructure is defined as $T_{TOT}(\omega) = u_N(\omega)/u_0(\omega)$.

Figures 6 and 7 compare responses of finite metastructures with $N = 10$ cells with integer and fractional-order resonators, for different values of damping in the base chain. The lightly-damped case, presented in Figure 6, is showcased to clearly present the behaviour of the system, however, if implemented, may lead to instability of a structure since the commensurate-order resonator is not negative imaginary and e.g. time delays if a digital implementation of the resonator is used. When such a system is implemented, the stability of not only unit cells in isolation, but complete metastructure should be validated. The structure in Figure 7 has a significant dampening and would yield a stable system even in presence of the aforementioned effects.

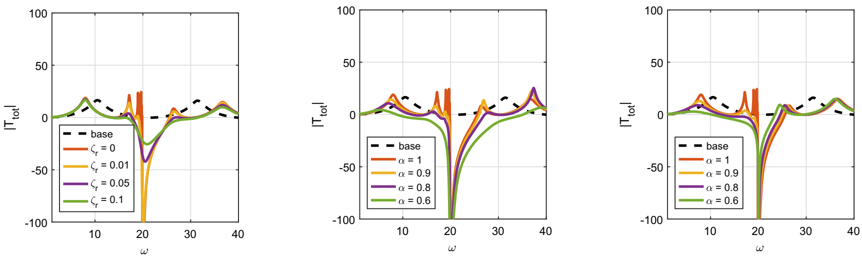

(a) $\alpha = 1$, $\zeta_p = 0.01$, $\zeta_r \neq 0$ (b) commensurate-order, $\zeta_p = 0.01$, $\zeta_{r,\alpha=1} = 10^{-6}$ (c) power-law, $\zeta_p = 0.01$, $\zeta_{r,\alpha=1} = 10^{-6}$

Fig. 7 Transmissablity of a finite metastructure of 10 cells with (a) integer-order and (b) commensurate-order or (c) power-law fractional-order resonators. The base chain of the metastructure has significant damping

In Figures 6a and 7a the effect of increasing the damping in the integer-order resonators is presented. As ζ_r increases, the resonance peaks created by the introduction of the resonators are damped, but with the price of increasing the vibration transmission within the band-gap region.

The use of commensurate-order resonators, presented in Figures 6b and 7b, reduces the undesired resonance peaks below and above the bandgap frequencies, without significant shallowing of the depth of the bandgap. Moreover, the bandgap expands as the order α is decreased. These effects are related to the dispersion diagram present in Figure 5b and the widening of the regions with $|\Im(\mu)| > 0$.

In the power-law FO case, presented in Figures 6c and 7c, the additional resonance peaks are attenuated only at lower frequencies, the bandgap region narrows down as α is decreased and the bandgap is not diminished significantly. All effects again correspond to the dispersion diagram in Figure 5c. In many applications, however, the disadvantages of the power-law element, when compared with the commensurate-order FO resonator, will be however outweighed by its stability properties, thanks to the phase of the element remaining between the low and high-frequency asymptotes. Moreover, when a bandgap is placed below the lowest resonance frequency of a finite host structure no additional resonance peaks above the bandgap frequencies are created [45, 46].

4 Conclusion

Elastic metamaterials with embedded resonators provide a promising approach to vibration isolation and attenuation. However, when resonators are applied to a finite host structure, not only the bandgap but also additional resonance peaks in its close vicinity are created. Increasing the damping of the resonator, which is a conventional approach for removing the undesired resonance peaks, results in shallowing of the bandgap region. We introduced an elastic metamaterial with fractional-order resonators and demonstrated that they can reduce the undesired resonances without significant changes to the maximal attenuation in the bandgap region. Both commensurate-order and power-law definitions of the fractional-order dynamics of the resonators were considered. The working principle of the proposed system was demonstrated on a single-unit cell and explained with the analysis of (pseudo)pole locations of the element. The properties of infinite metamaterial with FO resonators were studied using the dispersion method. Finally, we demonstrated that the fractional-order elements provide the desired effect by showcasing the transmissibility of a finite chain of unit cells. Analysis in this paper was limited to a granular metamaterial. While it can be expected that similar effects should be observed in other cases e.g. beams with translational resonators or piezoelectric patch actuators, detailed study is still required. The physical implementation of the studied elements also remains an open problem. While the FO resonators can be implemented as electronic or control elements, passive mechanical components with such dynamics still have to be developed.

Acknowledgements This work was supported by the NWO HTSM Applied and Technical Science Program under project MetaMech with number 17976.

Declarations

Conflict of interest The authors declare that they have no conflict of interest.

References

1. Adhikary, A., Sen, S., Biswas, K.: Practical realization of tunable fractional order parallel resonator and fractional order filters. IEEE Transactions on Circuits and Systems I: Regular Papers **63**(8), 1142–1151 (2016). https://doi.org/10.1109/TCSI.2016.2568262
2. Adolfsson, K., Enelund, M., Olsson, P.: On the fractional order model of viscoelasticity. Mechanics of Time-Dependent Materials **9**(1), 15–34 (2005). https://doi.org/10.1007/s11043-005-3442-1
3. Bonfanti, A., Kaplan, J.L., Charras, G., Kabla, A.: Fractional viscoelastic models for power-law materials. Soft Matter **16**(26), 6002–6020 (2020). https://doi.org/10.1039/d0sm00354a
4. Cajić, M., Karličić, D., Paunović, S., Adhikari, S.: A fractional calculus approach to metadamping in phononic crystals and acoustic metamaterials. Theoretical and Applied Mechanics **47**(1), 81–97 (2020). https://doi.org/10.2298/TAM200117003C
5. Caponetto, R., Dongola, G., Fortuna, L., Petráš, I.: Fractional Order Systems: Modeling and Control Applications. World Scientific Publishing Co. (2010). https://doi.org/10.1142/7709
6. Chang, I.L., Liang, Z.X., Kao, H.W., Chang, S.H., Yang, C.Y.: The wave attenuation mechanism of the periodic local resonant metamaterial. Journal of Sound and Vibration **412**, 349–359 (2018). https://doi.org/10.1016/j.jsv.2017.10.008
7. Chen, Y.Q.: Ubiquitous fractional order controls? In: IFAC Proceedings Volumes (IFAC-PapersOnline), vol. 2, pp. 481–492. Elsevier (2006). https://doi.org/10.3182/20060719-3-pt-4902.00081
8. Chen, Y.Q., Petráš, I., Xue, D.: Fractional order control - A tutorial. In: Proceedings of the American Control Conference, pp. 1397–1411 (2009). https://doi.org/10.1109/ACC.2009.5160719

9. Chen, Y.Y., Barnhart, M.V., Chen, J.K., Hu, G.K., Sun, C.T., Huang, G.L.: Dissipative elastic metamaterials for broadband wave mitigation at subwavelength scale. Composite Structures **136**, 358–371 (2016). https://doi.org/10.1016/j.compstruct.2015.09.048
10. Dastjerdi, A.A., Saikumar, N., HosseinNia, S.H.: Tuning guidelines for fractional order PID controllers: Rules of thumb. Mechatronics **56**, 26–36 (2018). https://doi.org/10.1016/j.mechatronics.2018.10.004
11. Dastjerdi, A.A., Vinagre, B.M., Chen, Y.Q., HosseinNia, S.H.: Linear fractional order controllers; A survey in the frequency domain. Annual Reviews in Control **47**, 51–70 (2019). https://doi.org/10.1016/j.arcontrol.2019.03.008
12. Den Hartog, J.P.: Mechanical Vibrations. McGraw-Hill Book Company Inc, New York (1940)
13. Ding, W., Hollkamp, J.P., Patnaik, S., Semperlotti, F.: On the fractional homogenization of one-dimensional elastic metamaterials with viscoelastic foundation. Archive of Applied Mechanics **93**(1), 261–286 (2023). https://doi.org/10.1007/s00419-022-02170-w
14. Feliu-Talegon, D., San-Millan, A., Feliu-Batlle, V.: Fractional-order integral resonant control of collocated smart structures. Control Engineering Practice **56**, 210–223 (2016). https://doi.org/10.1016/j.conengprac.2016.07.016
15. Frazier, M.J., Hussein, M.I.: Generalized Bloch's theorem for viscous metamaterials: Dispersion and effective properties based on frequencies and wavenumbers that are simultaneously complex. Comptes Rendus Physique **17**(5), 565–577 (2016). https://doi.org/10.1016/j.crhy.2016.02.009
16. Gantzounis, G., Serra-Garcia, M., Homma, K., Mendoza, J.M., Daraio, C.: Granular metamaterials for vibration mitigation. Journal of Applied Physics **114**(9), 093514 (2013). https://doi.org/10.1063/1.4820521
17. Ge, F., Chen, Y., Kou, C.: Cyber-physical systems as general distributed parameter systems: Three types of fractional order models and emerging research opportunities. IEEE/CAA Journal of Automatica Sinica **2**(4), 353–357 (2015). https://doi.org/10.1109/JAS.2015.7296529
18. Gómez-Aguilar, J.F., Rosales-García, J.J., Bernal-Alvarado, J.J., Córdova-Fraga, T., Guzmán-Cabrera, R.: Fractional mechanical oscillators. Revista Mexicana de Fisica **58**(4), 348–352 (2012). http://www.scielo.org.mx/scielo.php?script=sci_arttext&pid=S0035-001X2012000400010&lng=es&nrm=iso&tlng=enhttp://www.scielo.org.mx/scielo.php?script=sci_abstract&pid=S0035-001X2012000400010&lng=es&nrm=iso&tlng=en
19. Hussein, M.I., Leamy, M.J., Ruzzene, M.: Dynamics of phononic materials and structures: Historical origins, recent progress, and future outlook. Applied Mechanics Reviews **66**(4) (2014). https://doi.org/10.1115/1.4026911
20. Ivanova, E., Moreau, X., Malti, R.: Stability and resonance conditions of second-order fractional systems (2018). https://doi.org/10.1177/1077546316654790
21. Jiao, Z., Chen, Y.Q.: Stability of fractional-order linear time-invariant systems with multiple noncommensurate orders. Computers and Mathematics with Applications **64**(10), 3053–3058 (2012). https://doi.org/10.1016/j.camwa.2011.10.014
22. Kaczmarek, M.B., HosseinNia, H.: Fractional-order negative position feedback for vibration attenuation. Fractal and Fractional **7**(3), 222 (2023). https://doi.org/10.3390/fractalfract7030222
23. Kapoulea, S., Psychalinos, C., Elwakil, A.S.: Power law filters: A new class of fractional-order filters without a fractional-order Laplacian operator. AEU - International Journal of Electronics and Communications **129**, 153537 (2021). https://doi.org/10.1016/j.aeue.2020.153537
24. Kim, S.M., Wang, S., Brennan, M.J.: Comparison of negative and positive position feedback control of a flexible structure. Smart Materials and Structures **20**(1) (2011). https://doi.org/10.1088/0964-1726/20/1/015011
25. Laude, V.: Phononic Crystals: Artificial Crystals for Sonic, Acoustic, and Elastic Waves, 2nd Ed. De Gruyter (2020)
26. Liu, Y., Yu, D., Zhao, H., Wen, J., Wen, X.: Theoretical study of two-dimensional phononic crystals with viscoelasticity based on fractional derivative models. Journal of Physics D: Applied Physics **41**(6), 065503 (2008). https://doi.org/10.1088/0022-3727/41/6/065503
27. Ma, G., Sheng, P.: Acoustic metamaterials: From local resonances to broad horizons (2016). https://doi.org/10.1126/sciadv.1501595
28. Mahata, S., Herencsar, N., Kubanek, D.: On the design of power law filters and their inverse counterparts. Fractal and Fractional **5**(4), 197 (2021). https://doi.org/10.3390/fractalfract5040197
29. Malti, R., Moreau, X., Khemane, F., Oustaloup, A.: Stability and resonance conditions of elementary fractional transfer functions. Automatica **47**(11), 2462–2467 (2011). https://doi.org/10.1016/j.automatica.2011.08.029

30. Manimala, J.M., Sun, C.T.: Microstructural design studies for locally dissipative acoustic metamaterials. Journal of Applied Physics **115**(2), 023518 (2014). https://doi.org/10.1063/1.4861632
31. Marinangeli, L., Alijani, F., Hosseinnia, S.H.: Fractional-order positive position feedback compensator for active vibration control of a smart composite plate. Journal of Sound and Vibration **412**, 1–16 (2018). https://doi.org/10.1016/j.jsv.2017.09.009
32. Matignon, D.: Stability properties for generalized fractional differential systems. ESAIM: Proceedings **5**, 145–158 (1998). https://doi.org/10.1051/proc:1998004
33. Meral, M.E., Çelík, D.: A comprehensive survey on control strategies of distributed generation power systems under normal and abnormal conditions (2019). https://doi.org/10.1016/j.arcontrol.2018.11.003
34. Monje, C.a., Chen, Y.Q., Vinagre, B.M., Xue, D., Feliu, V.: Fractional-order Systems and Controls. Fundamentals and Applications. Springer-Verlag London Limited (2010). https://doi.org/10.1007/978-1-84996-335-0
35. Niu, W., Li, B., Xin, T., Wang, W.: Vibration active control of structure with parameter perturbation using fractional order positive position feedback controller. Journal of Sound and Vibration **430**, 101–114 (2018). https://doi.org/10.1016/j.jsv.2018.05.038
36. Oustaloup, A.: Systemes asservis lineaires d'ordre fractionnaire : theorie et pratique. Masson (1983)
37. Pang, D., Jiang, W., Liu, S., Jun, D.: Stability analysis for a single degree of freedom fractional oscillator. Physica A: Statistical Mechanics and its Applications **523**, 498–506 (2019). https://doi.org/10.1016/j.physa.2019.02.016
38. Radwan, A.G., Elwakil, A.S., Soliman, A.M.: On the generalization of second-order filters to the fractional-order domain. Journal of Circuits, Systems and Computers **18**(2), 361–386 (2009). https://doi.org/10.1142/S0218126609005125
39. Sahoo, S., Saha Ray, S., Das, S.: An efficient and novel technique for solving continuously variable fractional order mass-spring-damping system. Engineering Computations (Swansea, Wales) **34**(8), 2815–2835 (2017) https://doi.org/10.1108/EC-04-2016-0145. www.emeraldinsight.com/0264-4401.htm
40. San-Millan, A., Feliu-Batlle, V., Aphale, S.S.: Application of a fractional order integral resonant control to increase the achievable bandwidth of a nanopositioner. IFAC-PapersOnLine **50**(1), 14539–14544 (2017). https://doi.org/10.1016/j.ifacol.2017.08.2079
41. Schmidt, R.M., Schitter, G., Rankers, A., van Eijk, J.: The Design of High Performance Mechatronics, 2nd edn. IOS Press, Amsterdam (2014)
42. Sene, N., Aguilar, J.F.G.: Fractional mass-spring-damper system described by generalized fractional order derivatives. Fractal and Fractional **3**(3), 1–15 (2019). https://doi.org/10.3390/fractalfract3030039
43. Sepehri, S., Mashhadi, M.M., Fakhrabadi, M.M.S.: Wave propagation in fractionally damped nonlinear phononic crystals. Nonlinear Dynamics **110**(2), 1683–1708 (2022). https://doi.org/10.1007/s11071-022-07704-z
44. Singh, P.P., Roy, B.K.: Comparative performances of synchronisation between different classes of chaotic systems using three control techniques. Annual Reviews in Control **45**, 152–165 (2018). https://doi.org/10.1016/j.arcontrol.2018.03.003
45. Sugino, C., Leadenham, S., Ruzzene, M., Erturk, A.: On the mechanism of bandgap formation in locally resonant finite elastic metamaterials. Journal of Applied Physics **120**(13), 134501 (2016). https://doi.org/10.1063/1.4963648
46. Sugino, C., Xia, Y., Leadenham, S., Ruzzene, M., Erturk, A.: A general theory for bandgap estimation in locally resonant metastructures. Journal of Sound and Vibration **406**, 104–123 (2017). https://doi.org/10.1016/j.jsv.2017.06.004
47. Sugino, C., Ruzzene, M., Erturk, A.: Design and analysis of piezoelectric metamaterial beams with synthetic impedance shunt circuits. IEEE/ASME Transactions on Mechatronics **23**(5), 2144–2155 (2018). https://doi.org/10.1109/TMECH.2018.2863257
48. Sun, H., Du, X., Pai, P.F.: Theory of metamaterial beams for broadband vibration absorption. Journal of Intelligent Material Systems and Structures **21**(11), 1085–1101 (2010). https://doi.org/10.1177/1045389X10375637
49. Tavazoei, M.S., Haeri, M., Nazari, N.: Analysis of undamped oscillations generated by marginally stable fractional order systems. Signal Processing **88**(12), 2971–2978 (2008). https://doi.org/10.1016/j.sigpro.2008.07.002

50. Cao, K., Chen, Y., Stuart, D.: A fractional micro-macro model for crowds of pedestrians based on fractional mean field games. IEEE/CAA Journal of Automatica Sinica **3**(3), 261–270 (2016). https://doi.org/10.1109/JAS.2016.7508801
51. Tsirimokou, G., Psychalinos, C., Elwakil, A.S., Salama, K.N.: Electronically tunable fully integrated fractional-order resonator. IEEE Transactions on Circuits and Systems II: Express Briefs **65**(2), 166–170 (2018). https://doi.org/10.1109/TCSII.2017.2684710
52. Vinagre, B., Podlubny, I., Hernandez, A., Feliu, V.: Some approximations of fractional order operators used in control theory and applications. Fractional Calculus and Applied Analysis **3**(3), 231–248 (2000)
53. Voß, B., Weise, C., Ruderman, M., Reger, J.: Fractional-order partial cancellation of integer-order poles and zeros. IFAC-PapersOnLine **55**(25), 259–264 (2022). https://doi.org/10.1016/j.ifacol.2022.09.356
54. Wang, Z.H., Zheng, Y.G.: The optimal form of the fractional-order difference feedbacks in enhancing the stability of a sdof vibration system. Journal of Sound and Vibration **326**(3–5), 476–488 (2009). https://doi.org/10.1016/j.jsv.2009.07.003
55. Wang, G., Cheng, J., Chen, J., He, Y.: Multi-resonant piezoelectric shunting induced by digital controllers for subwavelength elastic wave attenuation in smart metamaterial. Smart Materials and Structures **26**(2), 025031 (2017). https://doi.org/10.1088/1361-665X/aa53ea
56. Zhang, S., Liu, L., Xue, D., Chen, Y.Q.: Stability and resonance analysis of a general non-commensurate elementary fractional-order system. Fractional Calculus and Applied Analysis **23**(1), 183–210 (2020). https://doi.org/10.1515/fca-2020-0007